Chapter 8

Innovative Applications of Ultrafine-Grained Materials

Jie Xu, Bin Guo and Debin Shan

Additional information is available at the end of the chapter

http://dx.doi.org/10.5772/intechopen.69503

Abstract

This chapter focuses on multifunctional properties of ultrafine-grained (UFG) metallic materials processed by severe plastic deformation (SPD), such as enhanced mechanical properties, excellent superplasticity, and wear resistance. Based on these multifunctional properties, the potential innovative application for UFG materials processed by SPD is introduced in the next section, including innovative application in micro-forming, nano-implants, electro-connections, and sport engineering.

Keywords: ultrafine-grained material, properties, micro-forming, MEMS

1. Introduction

Materials experts have asserted that materials breakthroughs in the twentieth century required about 20 years from the time of invention to gain widespread market acceptance [1]. Ultrafine-grained (UFG) materials are used as a structural material due to these properties. Bulk nanostructured metallic materials also have been following this track. Twenty-five years ago, in 1988, there appeared a classic description of the application of severe plastic deformation (SPD) to bulk solids in order to achieve exceptional grain refinement to the submicrometer level [2]. Though a wide research started at the beginning of 1990, a great progress in commercial applications of UFG materials has been made just in the last few years. This chapter focused on multifunctional properties of ultrafine-grained metallic materials, including mechanical properties, superplasticity, wear resistance, etc. The innovative application of UFG materials was introduced in the following section, including in micro-forming and other commercial industries.

2. Multifunctional properties of ultrafine-grained materials

2.1. Enhanced mechanical properties

The grain size, d, plays a dominant role on the strength of polycrystalline metallic materials according to the Hall-Petch equation which states that the yield stress, σ_y, is given by [3, 4]

$$\sigma_y = \sigma_0 + k\, d^{-1/2} \tag{1}$$

where σ_0 is the friction stress and k is the Hall-Petch constant [1]. It follows from Eq. (1) that the strength increases with a decrease of grain size, and this leads to an ever-increasing interest in producing UFG materials with grain size of submicrometer or even nanometer level, which are processed by severe plastic deformation (SPD) techniques, including equal-channel angular pressing (ECAP) and high-pressure torsion (HPT). This means that UFG materials are anticipated to exhibit exceptional strength according to the Hall-Petch equation in Eq. (1).

For example, **Figure 1** shows the average Vickers microhardness values which were taken over the total surface of each disk for the AZ31 magnesium alloy processed by ECAP for up

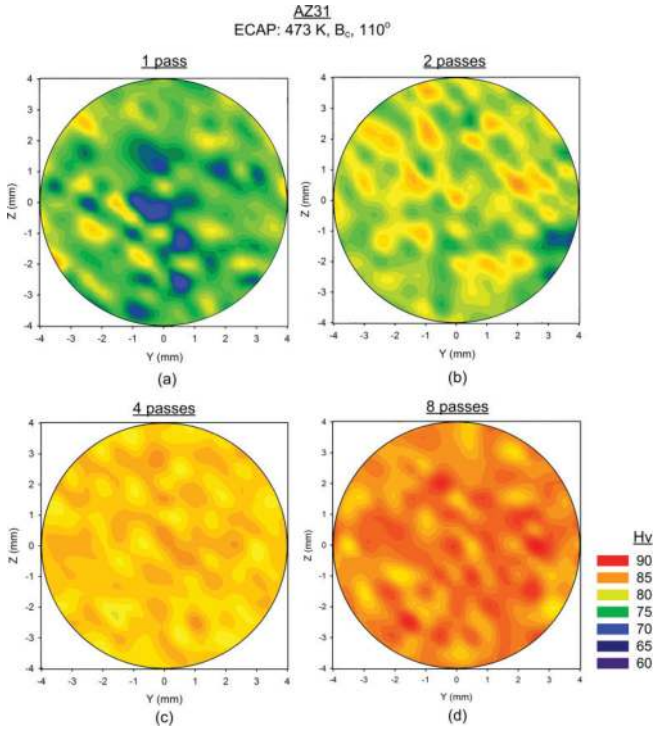

Figure 1. Distribution of microhardness of AZ31 processed by ECAP through (a) one pass, (b) two passes, (c) four passes, and (d) eight passes [5].

to eight passes [5]. The results demonstrate that the average value of the microhardness, Hv, increases significantly after one pass and continues to increase slowly up to eight passes. It is apparent in **Figure 1** that the samples processed by ECAP through one and two passes exhibit a higher average microhardness over the entire surface than the as-received sample as shown in **Figure 1(a)** and **(b)**. After four passes of ECAP, the sample achieves a reasonable level of homogeneity over the plane as shown in **Figure 1(c)**, and finally there is additional hardening and a general homogeneity after ECAP for eight passes in **Figure 1(d)**. These microhardness results demonstrate that the strength can be enhanced significantly by ECAP processing.

By comparison with the sample processed by ECAP, **Figure 2** shows the evolution in microhardness over one-quarter of the disk for the same AZ31 alloy processed by HPT through (a) 1/4, (b) 1, (c) 5, and (d) 10 turns [6]. There is a gradual evolution toward higher microhardness values with increasing numbers of turns after HPT processing. There is a reasonable level of hardness homogeneity which is achieved across the HPT disks through ten turns with a saturation hardness value of Hv ≈ 125 as shown in **Figure 2** [6]. This gradual development of hardness homogeneity is consistent with several experimental reports for magnesium alloys processed by HPT [7–10]. There are many other papers reporting the enhanced strength of UFG materials processed by SPD methods [11–15].

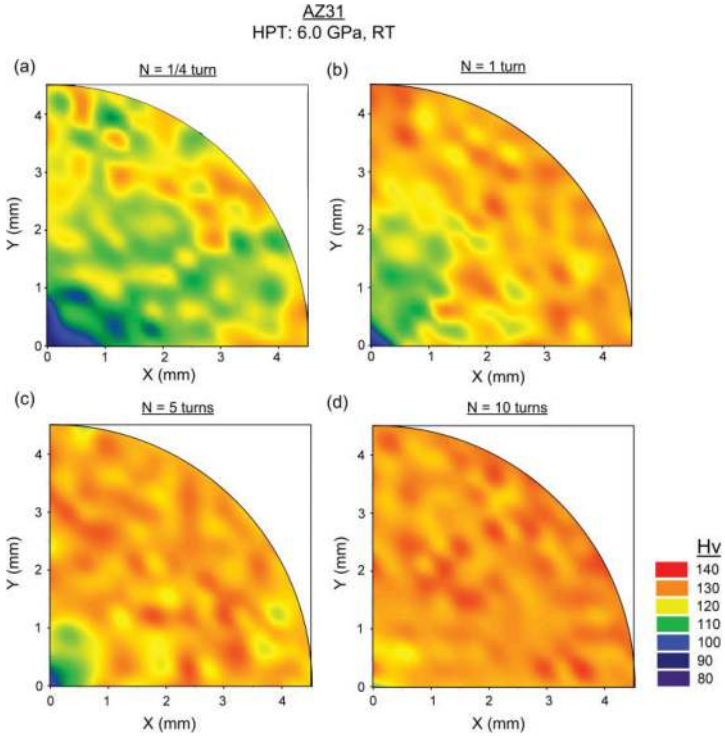

Figure 2. The variation of microhardness over one-quarter area of the disks processed by HPT through (a) 1/4, (b) 1, (c) 5, and (d) 10 turns[6].

High ductility in metallic materials is another very important property, which is essential for metal-forming operations as well as to avoid catastrophic failure in load-bearing applications during their service life. However, most of the UFG materials processed by SPD demonstrate significantly higher strength than the coarse-grained (CG) counterparts but have a relatively low ductility. Various strategies to improve low ductility of the UFG materials have been proposed, which can be divided into two groups of "mechanical" strategies and "microstructural" strategies [16, 17]. For example, there are different finds of strength and ductility in high-purity Cu with initial coarse grains, cold rolling (CR) with reduction ratio of 60%, and after ECAP processing up to 16 passes. The results for the ECAP-processed Cu demonstrate an enhanced strength with good ductility similar to the CG sample [12]. As shown in **Figure 3**, for Cu and Al, CR (the reduction in thickness is marked by each datum point) increases the yield strength but decreases the elongation to failure [18, 19]. The extraordinary combination of high strength and high ductility shown in **Figure 3** for the nanostructured Cu and Ti after SPD processing clearly sets them apart from the other CG metals [20].

2.2. Excellent superplasticity

Superplasticity is a well-recognized mechanical property in polycrystalline metallic materials that have the ability to pull out to a very high elongation without any significant necking in tension. The superplastic flow mechanism is dominated by the process of grain boundary sliding (GBS) in which the small grains slide over each other in response to the applied stress [21]. The GBS needs intragranular slip as an accommodation mechanism, and this slip

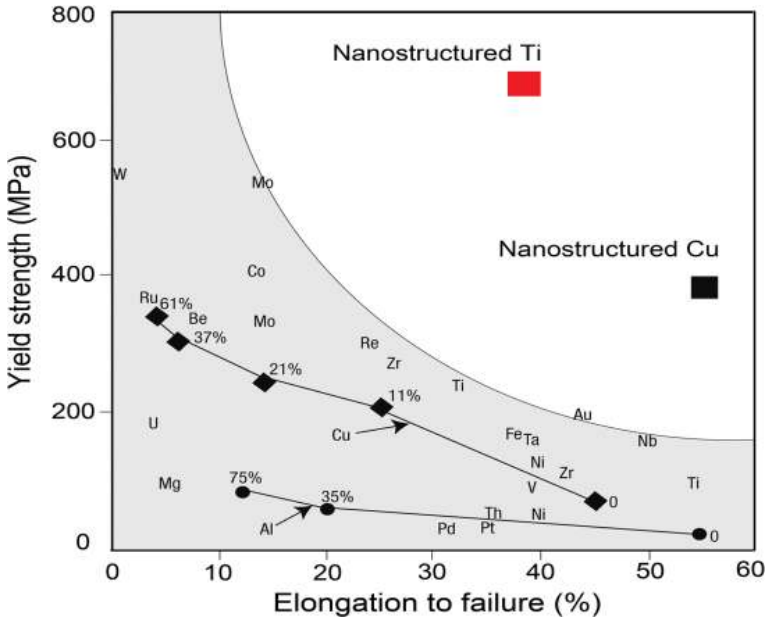

Figure 3. The extraordinary combination of high strength and high ductility in metals processed by SPD [20].

is held up at subgrain boundaries in CG materials. Accordingly, the UFG materials processed by SPD have an opportunity to achieving good superplasticity due to submicrometer grain size with high fraction of high-angle boundaries [22–32].

For example, there is no superplasticity after cold rolling (CR) because of the presence of low-angle sub-boundaries. By comparison, the presence of UFG structures can lead to exceptional superplasticity at elevated temperatures. An excellent superplasticity in an UFG Al-3% Mg-0.2% Sc alloy after processing by ECAP through eight passes was found, and the maximum elongation of 2280% can be obtained after tension tests at strain rate of 3.3×10^{-2} s^{-1} and the temperature of 673 K [33]. The highest elongation of 3030% was recorded after tension at a strain rate of 1.0×10^{-4} s^{-1} and the temperature of 473 K in a ZK60 Mg-5.5% Zn-0.5% Zr alloy processed by extrusion and ECAP as shown in **Figure 4** [34]. This is the highest elongation in a Mg alloy processed under any condition and one of the highest elongations recorded in any materials processed by ECAP [35]. In addition, the absence of any visible necking within the gauge length in **Figure 4** demonstrates conclusively that this is a true superplastic flow [36].

Processing by HPT can also produce UFG materials that have a potential for achieving superplastic elongation in tension. An example is shown in **Figure 5** for the superplasticity in

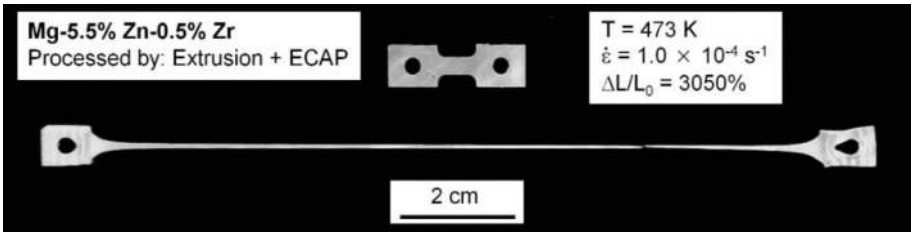

Figure 4. Exceptional superplasticity in a ZK60 alloy processed by ECAP [34].

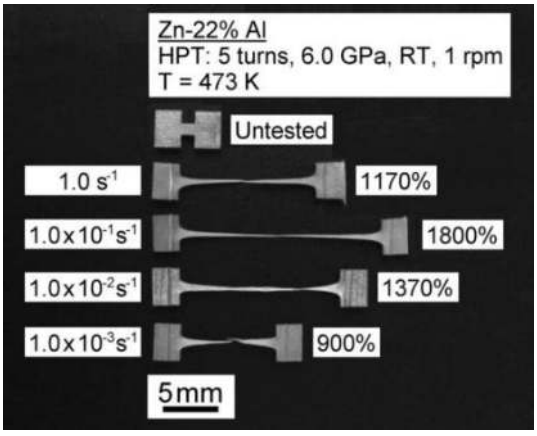

Figure 5. Superplasticity in the Zn-22% Al alloy after processing by HPT [37].

tension at 473 K using different strain rates in a Zn (22%)-Al alloy processed by HPT through five turns at room temperature under an applied pressure of 6.0 GPa [37]. It is evident from **Figure 5** that very high elongations may be achieved at strain rates in the vicinity of 10^{-1} s^{-1}, whereas there is a clear evidence for necking in the two samples pulled at the slowest strain rates. A tabulation of superplastic data for samples prepared by HPT shows that the elongation of 1800% visible in **Figure 5** is the highest elongation reported to date for any material processed by HPT [37]. However, the highest elongation in the same UFG Zn-22% Al alloy processed by ECAP occurs at 10^{-2} s^{-1} [38]. High strain rate superplasticity can be achieved by using ECAP or HPT. Compared with the sample processed by ECAP, the optimum superplasticity for the sample processed by HPT correctly occurs at faster strain rate, but maximum elongation is reduced. The elongation is reduced because HPT samples have very small gauge sections.

In the recent report, there is an instructive comparison of the superplasticity in various materials processed by ECAP and HPT with other processing techniques as shown in **Figure 6** [39], where the superimposed on each diagram are the appropriate ranges for UFG Al alloy processed by ECAP and HPT indicated by the dashed ovals fill in the diagrams first developed 20 years ago [40]. It is readily apparent from **Figure 6** that both the ECAP and HPT processing methods extend the plastic forming rate of the given materials with faster strain rates and higher elongation. The expanded ranges generally overlap with the ranges associated with powder metallurgy (PM) materials. This expansion in the range of strain rate reveals an important advantage for the SPD processing without any contamination and/or porosity

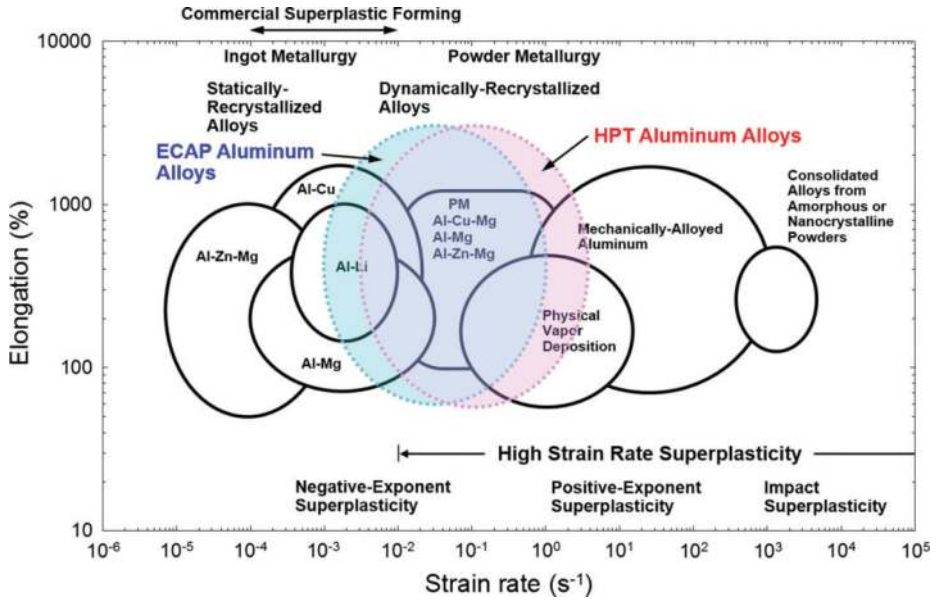

Figure 6. A plot of elongation versus strain rate for a series of Al alloys produced using different processing methods [39].

in using PM methods. Thus, processing of SPD techniques demonstrates a very important approach for extending the future applications of numerous simple metals and alloys [39].

2.3. Wear resistance

Wear resistance is an important property for UFG materials in order to evaluate their potential for use as structural components [41]. The wear of sliding surfaces can occur by one or more wear mechanisms, including adhesion, abrasion, fatigue wear, corrosive wear, and fretting. For the metallic materials, the wear volume under abrasive and some adhesive wear models is generally assumed to be inversely proportional to the hardness of the materials according to the traditional Archard relationship which is given by [42]

$$V = K\frac{LN}{H} \tag{2}$$

where V is the wear loss of the volume, N is the applied force, L is the sliding distance, K is the wear coefficient, and H is the hardness on wear surface of the material. Because the UFG materials processed by SPD techniques normally have much higher hardness values than the conventional CG materials, it is critical to have superior wear resistance for UFG materials. However, there has been a disagreement in this regard among researchers [41].

There are a number of studies reporting an improved wear resistance in UFG materials produced by ECAP and HPT. For example, the dry sliding wear tests of an aluminum alloy processed by ECAP method showed that the wear mass loss decreased significantly with increasing of the numbers of ECAP passes [43]. A similar enhanced wear resistance property was also presented in an Al-Mg-Si alloy processed by ECAP [44]. An investigation of friction and wear behavior revealed that grain size was the important factor determining the transition from elasto-hydrodynamic lubrication to the boundary lubrication regions [45, 46]. An investigation of the aluminum bronze alloy processed by ECAP demonstrated that the coefficient of friction decreased with increasing numbers of ECAP passes and accordingly the wear resistance was improved significantly after ECAP processing [47, 48]. Similarly, a characterization of the dry sliding wear behaviors of Cu-0.1 wt.% Zr alloy and AZ31 alloy processed by ECAP was investigated [49, 50], and the wear volume loss of the samples processed by ECAP becomes much lower than the annealed alloy as shown in **Figure 7** due to the higher microhardness introduced by ECAP processing [49]. Processing by ECAP can produce bulk materials with significantly enhanced mechanical properties due to the grain refinement, and therefore the wear loss of the ECAP-processed alloy is much smaller than for the annealed alloy. Some papers are now available on the wear behavior of commercial purity Ti processed by HPT method. Compared with the CG pure Ti, the wear resistance of pure Ti processed by HPT was improved significantly both in dry and wet sliding tests [51, 52].

On the other hand, there are also some other contradictory results on wear property in UFG materials. For example, the wear resistance of some UFG materials processed by ECAP was lower than for the as-received CG materials [53]. For example, the dry sliding wear tests of an Al-1050 alloy were conducted with the as-received condition and UFG materials with grain size of ~1.3 μm after ECAP processing through eight passes [54]. The UFG samples

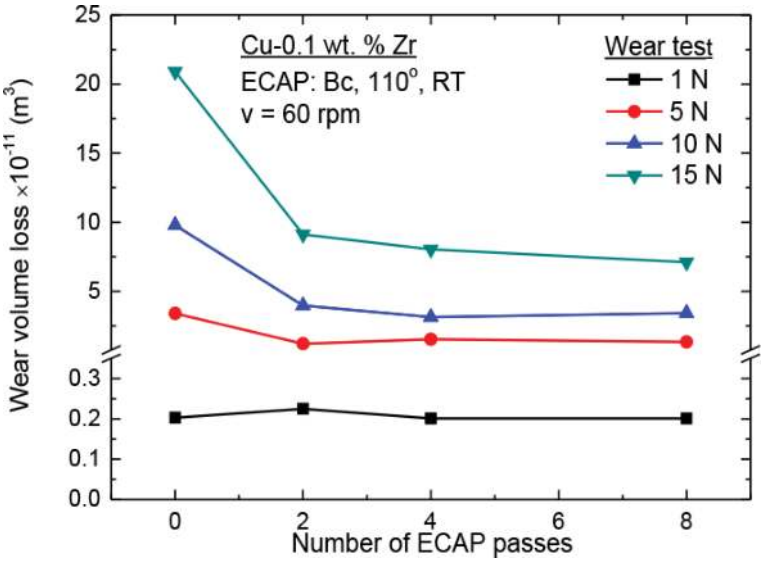

Figure 7. The wear volume loss versus the number of ECAP passes for a sliding time of 600 s under normal loads of 1, 5, 10, and 15 N.

have a similar coefficient of friction (COF) and the higher wear loss than the as-received sample although the microhardness value is improved significantly after ECAP processing. An investigation of UFG AISI 1024 steel processed by a warm multiaxial forging technique showed that there is no obvious improvement on wear resistance property though the strength property can be enhanced significantly due to the effects of higher density of grain boundaries and submicrometer-sized cementite particles [55]. There is a surprising result that there is no corresponding improvement in the wear resistance in pure titanium processed due to the occurrence of oxidative wear with an abrasive effect [56]. As a consequence of these varying reports, it is readily apparent that further investigations should be further conducted in order to evaluate the wear behavior of UFG materials processed by SPD techniques.

3. Innovative application of ultrafine-grained materials

It is well established that SPD techniques are very effective in producing UFG materials with submicrometer or even nanoscale grain sizes, and these materials have superior mechanical properties including high strength and, if the fine grains are reasonably stable, a good superplastic capability at elevated temperatures [57, 58]. Despite a wide research on SPD techniques started at the beginning of 1990, very significant progress in the commercialization of UFG materials has been made in the recent years. In this section, the innovative application of UFG metallic materials processed by SPD is discussed.

3.1. Potential application in micro-forming technology

Micro-forming is defined as the production of parts or structures having at least two dimensions in the submillimeter range, which becomes an attractive option in the manufacturing of these products because of its advantages for mass production with controlled forming quality, high production rate, and low cost [59–61]. Nevertheless, although the knowledge of tool design and fabrication techniques are now well developed for the conventional macro-forming, there is an evidence that the occurrence of size effects may lead to a breakdown in these basic plastic deformation theory when the specimen dimensions are scaled down to the micro/mesoscale [62, 63]. In practice, if there are only a few grains in the micro-parts, the response to the applied forces will show significant variations, and the reproducibility of the mechanical properties will become a serious problem in any micro-forming processes [64]. Hopefully, there is a way to solve grain size effects in micro/mesoforming by applying UFG materials with submicrometer or even nanoscale grain sizes produced by SPD techniques [65–68] because ultrafine grains can improve the micro-formability, surface roughness, and good mechanical properties of the MEMS components [69–71].

However, micro-deformation behavior changes from dislocation dominated in large grains to grain boundary dominated in small-grain regimes when the grain size decreases to the submicron range. For example, the deformation behavior in UFG pure aluminum processed by ECAP and post-annealed specimens at room temperature (RT) was investigated, and the results show that different work hardening behaviors were observed during macro-compression test when the grain size increased from 0.35 to 45 μm [72]. The strain rate also has an obvious effect on micro-compression behavior of UFG pure aluminum, and the results demonstrate that a lower strain rate causes activation of micro-shear banding [73], and the deformation mechanism may be related to grain boundary sliding in UFG pure aluminum [74]. Thus, it is believed that grain boundary sliding and grain rotations are the main deformation mechanism in the UFG materials processed by SPD techniques. However, there is only limited information available on micro-forming when the material grain size is reduced to the submicrometer even nanoscale level although these problems and limitations are beginning to attract attentions within the materials science community. At the present time, Le et al. [75] investigated the influence of grain size ranging from 0.5 to 5.2 μm on the deformation behavior by compression tests at macroscale in aluminum prepared by a spark plasma sintering method. The results indicate that there is a strong correlation between deformation microstructure and grain size in the micrometer regime. Okamoto et al. [76] investigated the specimen and grain size effects on micro-compression formation behavior in the electrodeposited nanocrystalline copper with average grain size of 360, 100, and 34 nm. The results show that the deformation mechanisms with nanocrystalline grains are different from those for pillar with submicron grain size from the surface microstructure of deformed micropillars. There is a significant micro-deformation difference between the CG and UFG materials. For example, the micro-deformation behavior is transferred from work hardening to slight strain weakening with decreasing of grain size during micro-compression. The microstructural evolution results show that a lot of low-angle grain boundaries and recrystallized fine grains are formed inside of the original large grains in CG pure aluminum. By contrast, ultrafine grains are

kept in UFG pure aluminum, which are similar to the original microstructure before micro-compression. Meanwhile, there is an obvious transition from nonuniform deformation to uniform deformation after micro-compression testing with decreasing of grain size as shown in **Figure 8a–e**. The nonuniform deformation can be improved significantly, and the compressed specimens using UFG pure Al are cylindrical with a smooth surface as shown in **Figure 8d** and **e** [77, 78]. Research on the micro-extrusion of UFG aluminum showed that the material flow became more uniform because more grains were deformed during micro-extrusion [79]. Similarly, an investigation of the effect of specimen size on tensile testing with UFG and CG pure copper demonstrates that the uniform elongation increases with increasing specimen thickness and decreasing gauge length. In addition, the failure mode changed gradually from shear to normal tensile failure with increasing of specimen thickness [80, 81]. Therefore, the surface roughness and coordinated deformation ability can be significantly improved during micro-compression with UFG materials, which demonstrates that they have a potential application in micro-forming at ambient temperature.

The ductility at micro/mesoscale is another method to evaluate the UFG materials whether the alloy has the potential for use in micro-forming applications. The mechanical properties confirm the general behavior anticipated for UFG metals including a strengthening at ambient temperature through the Hall-Petch relationship and a decrease in yield stress and higher ductilities when testing at elevated temperatures. For example, an investigation of the superplastic micro-forming of the magnesium AZ91 alloy with a UFG microstructure showed that the grain size and the transition from superplastic flow to non-superplastic flow were the main parameters controlling the micro-formability [82]. A UFG AZ31 magnesium alloy with average grain size of ~110 nm processed by HPT for 10 turns under an imposed pressure of 6.0 GPa shows a highest elongation of ~400% testing at a temperature of 423 K and a strain rate of 1.0×10^{-4} s^{-1} [6]. This elongation of the sample processed by HPT is more than two times larger than the elongation of ~192% recorded in the same alloy processed by ECAP through eight passes testing at 472 K [5]. Thus, the micro-tensile testing of the UFG AZ31 magnesium

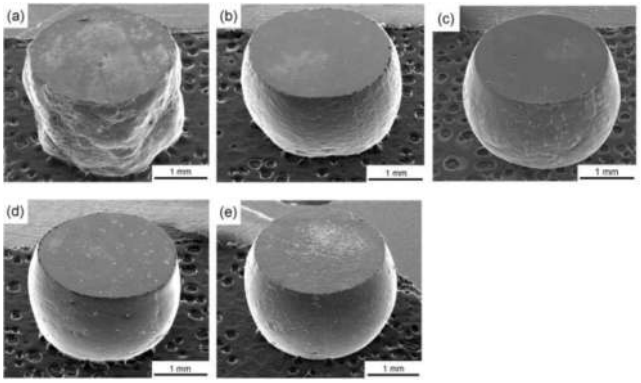

Figure 8. Surface topographies of the compressed sample with grain size of (a) ~150, (b) ~25, (c) ~4, (d) ~1.5, and (e) ~1.3 μm when compressed with fixed specimen diameter 2 mm [77].

alloy processed by HPT suggests the possibility of obtaining a true superplastic property at a testing temperature which is much lower than for the same samples processed by ECAP.

To evaluate the micro-formability of UFG materials, a micro-V-groove die with a width of 100 μm and the V angle of 60° was proposed as shown in **Figure 9** [83]. The micro-coining tests were conducted with the as-drawn and UFG AZ31 magnesium alloy at the temperatures ranging from 298 to 523 K. After micro-coining tests, the surface shape of the embossed specimen was measured, and the filling area Af was calculated from the measurement data. The filling ratio Rf of the filling area Af to the V-groove area Av was used to evaluate the formability after micro-embossing. **Figure 9** shows the different filling behaviors during micro-coining with the as-drawn AZ31 magnesium alloy and UFG AZ31 alloy processed by HPT. For the as-drawn AZ31 magnesium alloy, the percentage of flowed area, Rf, increases slowly with increasing temperature from room temperature to 423 K and then increases abruptly up to 523 K. In contrast, the filling ratio, Rf, increases significantly when the embossing temperature in UFG AZ31 is elevated from 298 to 423 K and then continues to increase slowly with increasing of embossing temperature up to 523 [84]. Thus, UFG AZ31 alloy processed by HPT exhibits an excellent micro-formability by superplastic deformation, which is expected to become one of most useful materials to fabricate MEMS components with complicated structures.

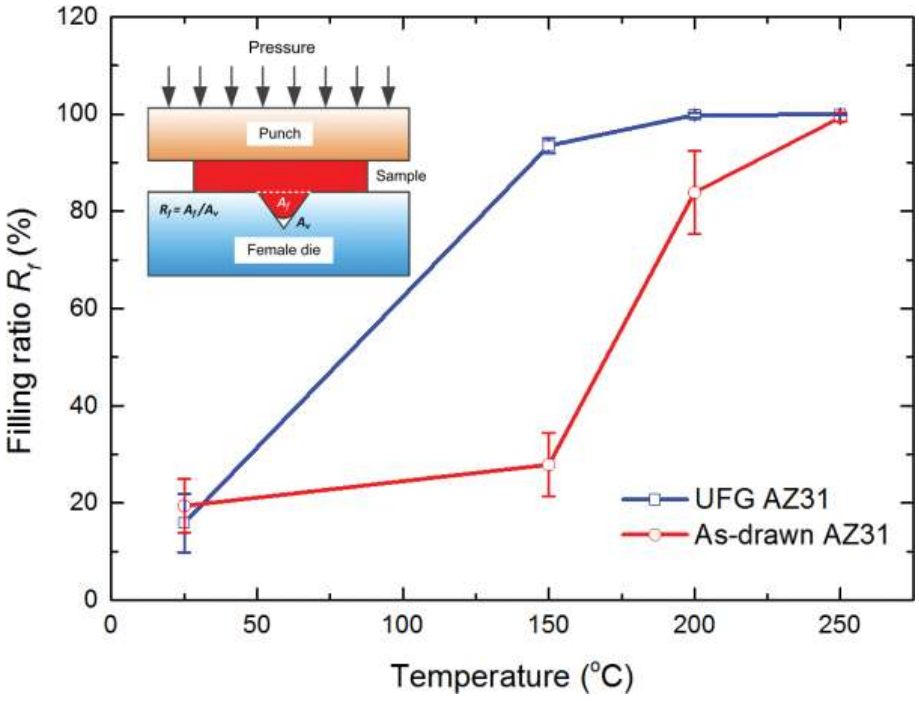

Figure 9. Plots of filling ratio versus the increasing of embossing temperature for UFG AZ31 alloy processed by HPT and as-drawn AZ31 alloy [83].

Based on these results, it is concluded that the SPD-processed UFG materials have a strong potential for use in micro-forming applications at elevated temperature. For example, a UFG pure Al with average grain size of ~1.0 μm produced by ECAP was adopted for micro-hot-embossing processes using a novel micro-embossing tool that was designed with a self-adaptive adjustment and a vacuum mounting system [84]. The microarray channels are fabricated with feather widths from 5 to 100 μm at the temperature of 523 K under a force of 4 kN followed by a dwell time of 600 s as shown in **Figure 10**. The embossed micro-channels of 100 μm in width are clearly formed with a good geometrical transferability and no obvious defects as shown in **Figure 10a**. The straight side walls are replicated from the micro-silicon dies, but the top surface becomes rough and even with the decreasing of channel widths, as shown in **Figure 10b–d**. These results demonstrate that the filling quality is mainly attributed to the channel dimension compared to the grain size at the given micro-embossing conditions [84].

Figure 11 shows the comparison of the profile measurements for the micro-channels that are 25 μm in width were embossed under the same experimental conditions using CG pure Al and UFG pure Al after ECAP processing through eight passes [84]. The filling problem of CG pure Al with an average grain size of ~300 μm is much more serious for micro-embossing at 25 μm in width because there are some wrinkles and uneven channels after micro-embossing. During the micro-embossing tests of the CG pure Al, the micro-channel on the silicon die is filled by a single grain deformation in the transverse direction because the grain size of CG pure Al is much larger than the channel width. So the material flow behavior is different at the grain boundary and at the edge of the micro-channels, which leads to an inclined surface and wrinkles. By contrast, the micro-embossing of UFG pure Al at the same temperature produces smooth micro-channels, and the patterns on the silicon mold are fully transferred to the UFG pure Al plate. These results demonstrate that the UFG pure Al has much better formability than the CG pure Al. Therefore, micro-hot-embossing of UFG pure Al has good potential for application

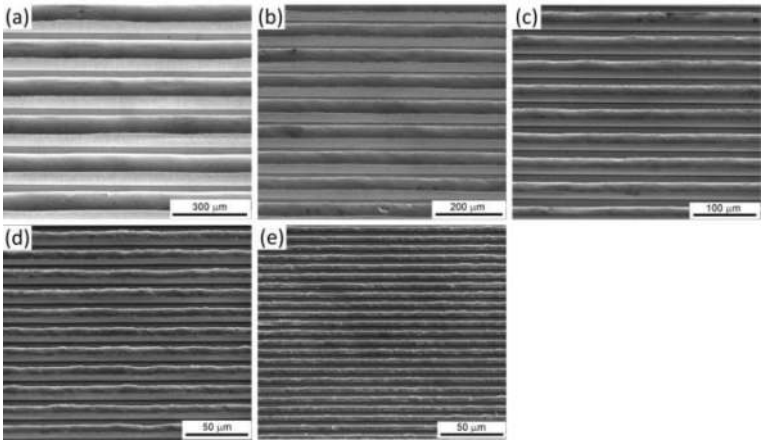

Figure 10. SEM images of microarray channels with sizes of (a) 100, (b) 50, (c) 25, (d) 10, and (e) 5 μm in width [84].

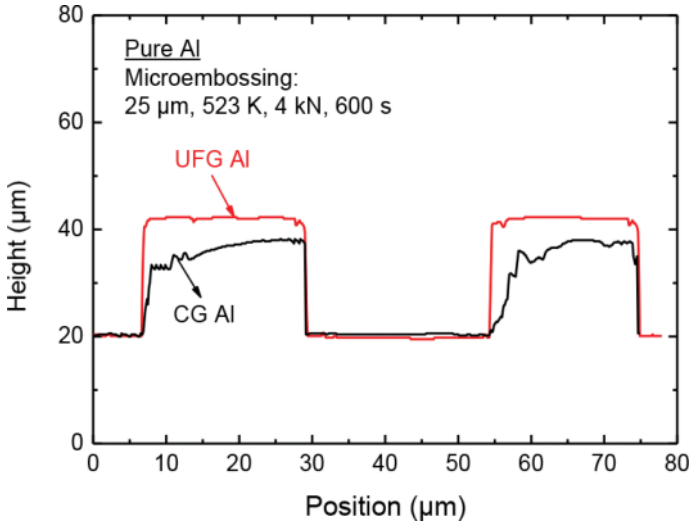

Figure 11. Comparison of the filling quality using UFG and CG pure Al [84].

in the fabrication of micro-parts with the micro-forming mold equipped with self-adaptive adjustment and a vacuum mounting system [84].

The UFG materials processed by SPD appear to provide a significant potential for use in micro-forming applications at elevated temperatures due to their enhanced mechanical properties at the room temperature and improved ductility at the elevated temperatures. However, the present investigation demonstrates that there is also an excellent micro-formability when using UFG pure aluminum at ambient temperature. The micro-tensile testing shows that the UFG pure Al processed by ECAP has excellent mechanical properties compared with the CG pure Al. The highest elongation of ~72% after ECAP processing suggests a good potential for using this material in micro-forming process at ambient temperature [85]. Moreover, micro-compression testing shows that the UFG pure Al produced by ECAP has improved the deformation compatibility by comparison with the CG sample and benefits to filling quality during micro-forming. This was confirmed by successfully using micro-forming to fabricate a micro-turbine from UFG pure aluminum at ambient temperature as shown in **Figure 12**. The perfection of this micro-turbine is a direct consequence of the high forming quality and the generally uniform mechanical properties of this material. The high strength and high level of homogeneity are also confirmed directly by microhardness measurements. These results demonstrate that there is an excellent potential for using UFG materials to fabricate micro-parts with high accuracy, high strength, and a high level of uniformity [85].

3.2. Commercial applications of ultrafine-grained materials

Application and commercialization of UFG materials are associated with three primary points: their superior properties, their efficient fabrication, and the possibility to produce

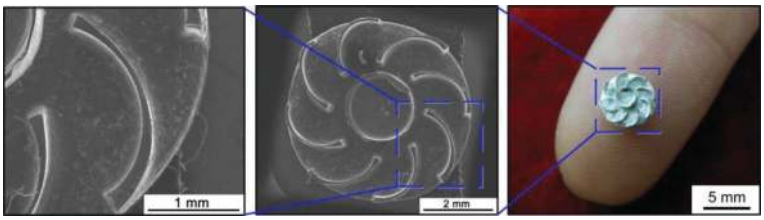

Figure 12. Micro-turbine of UFG pure aluminum formed at ambient temperature [85].

cutting-edge products from these materials [86]. Below are the examples of UFG materials processed by SPD for their commercial applications in biomedical engineering, electrical engineering, and sports.

The UFG pure titanium processed by ECAP-Conform from the Ufa State Aviation Technical University under the management of professor Valiev has been used as trademark application to manufacture dental implants in the company "Timplant" (Ostrava, Czech Republic) since 2006 [87]. The UFG Ti with ultimate strength of 1350 MPa enabled design of thin dental implant with diameter of 2.0 mm, which serves as fully functional pillar, and it can be inserted into very thin bones. Another advantage of smaller dental implants is less damage induced into jawbone during surgery intervention [88]. To date, these dental implants have been certified according to the European standard EN ISO 13485:2003. **Figure 13a** illustrates the Nanoimplant®, which is installed into the body of an 18-year-old patient with thin jawbones between teeth 11 and 13. Another implant with the diameter of 2.4 mm was inserted to the right-side position 12 as shown in **Figure 13b** and **c**. Two nanoimplants with two temporary crowns made in the same day as implants were inserted in the patient left the dental office. After 6 weeks, the final metal-ceramic crowns were fixed on the implants [89]. One of the possible next dental implant products with UFG Ti produced by SPD was manufactured and sold by basic implant systems under the trademark Biotanium in the USA beginning in 2011 [86]. Thus, the small-diameter dental implants made from UFG Ti are possible to replace standard ones made from Ti-4Al-6V alloy, since the UFG pure Ti is characterized not only by the improved mechanical strength and fatigue life but also by better biocompatibility compared to the conventional Ti-4Al-6V alloy.

UFG pure copper, aluminum, and aluminum alloy would be an innovative solution for electro-connections in high-voltage current converter due to the improved mechanical property without reduction of their electrical conductivity or even with its significant improvement. For example, very thin Cu and Al-2% Fe wires with a final diameter of 0.08 mm were successfully drawn from the ring sample processed by HPT for N = 1 revolution as shown in **Figure 14** [90]. A 25:1 area reduction after wire drawn can be achieved from the HPT processed samples, but the wire draw from the as-cast state failed after 12:1 reduction [90]. The electrical conductivity of the wires ranges from 49–51 IACS% and increased to 52–54% after aging at 473 K for 1 h. These results demonstrate that there is a large potential to further improve the electrical conductivity with an optimized aging treatment [91].

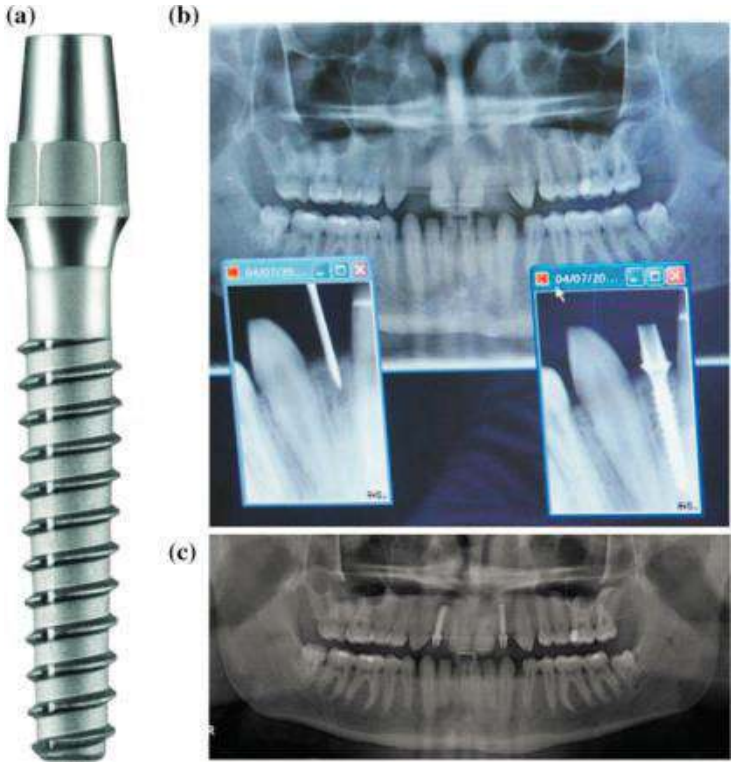

Figure 13. (a) Dental implant from nanostructured Ti and (b and c) X-ray photographs after surgery and control photograph after incorporation of dental implants into human jaw [89].

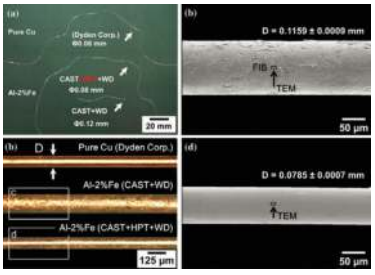

Figure 14. (a) Photograph and (b) optical micrograph of pure Cu and Al-2 % Fe as-drawn wires. SEM images showing surface condition of wires drawn from c as cast state and d HPT-processed state [90].

Producers of sport devices/equipment can also benefit from the UFG metals, particularly where high strength and low weight are required. The UFG materials could find applications in high-performance golf, bicycles, tennis, hockey, mountain equipment, etc. One of

Figure 15. Components of golf club made from nanostructured Ti-6Al-4V alloy [93].

the important examples is nano-dynamic high-performance golf balls, which have a hollow nanostructured titanium core. The core material is manufactured using the UFG chip from Purdue University [92]. The Institute for Metals Superplasticity Problems (Russia) has developed a technology for the fabrication of golf club components from UFG Ti-6Al-4V alloy with grain size of 200 nm as shown in **Figure 15** [93]. The method for producing the goffer-type face using UFG or nanostructured metals and inserts provided processing faces characterized by enhanced strength and high-impact efficiency. This technology allowed a reduction in weight of a golf club along with increase of ball's flight distance due to increased restitution factor [93]. These application results demonstrate wide commercial potentialities for applying UFG materials processed by SPD.

Author details

Jie Xu*, Bin Guo and Debin Shan

*Address all correspondence to: xjhit@hit.edu.cn

Harbin Institute of Technology, Harbin, China

References

[1] Eagar T. Bringing new materials to market. Technology Review. 1995;98:42-49

[2] Langdon TG. Twenty-five years of ultrafine-grained materials: Achieving exceptional properties through grain refinement. Acta Materialia. 2013;61:7035-7059

[3] E.O. Hall. The deformation and ageing of mild steel: III discussion of results. Proc. Phys. Soc. Lond. B 1951;**64**:747-752

[4] N.J. Petch. The cleavage strengh of polycrystals. J. Iron. Steel. Inst. 1953;**174**:25-28

[5] Xu J, Shirooyed M, Wongsa-Ngam J, Shan D, Guo B, Langdon TG. Hardness homogeneity and micro-tensile behavior in a magnesium AZ31 alloy processed by equal-channel angular pressing. Materials Science and Engineering: A. 2013;**586**:108-114

[6] Xu J, Wang X, Shirooyed M, Xing G, Shan D, Guo B, Langdon TG. Microhardness, microstructure and tensile behavior of an AZ31 magnesium alloy processed by high-pressure torsion. Journal of Materials Science. 2015;**50**:7424-7436

[7] Vrátná J, Janeček M, Čížek J, Lee DJ, Yoon EY, Kim HS. Mechanical properties and microstructure evolution in ultrafine grained AZ31 alloy processed by severe plastic deformation. Journal of Materials Science. 2013;**45**:4705-4712

[8] Kawasaki M, Figueiredo RB, Huang Y, Langdon TG. Interpretation of hardness evolution in metals processed by high-pressure torsion. Journal of Materials Science. 2014;**49**:6586-6596

[9] Malheiros LRC, Figueiredo RB, Langdon TG. Grain size and microhardness evolution during annealing of a magnesium alloy processed by high-pressure torsion. Journal of Materials Research and Technology. 2015;**4**:14-17

[10] Vrátná J, Janeček M, Gubicza J, Krajňák T, Yoon EY, Kim HS. Evolution of microstructure and hardness in AZ31 alloy processed by high pressure torsion. Materials Science and Engineering: A. 2015;**625**:98-106

[11] Furukawa M, Horita Z, Nemoto M, Valiev RZ, Langdon TG. Factors influencing the flow and hardness of materials with ultrafine grain sizes. Philosophical Magazine A. 1998;**78**:203-216

[12] Valiev RZ, Alexandrov IV, Zhu YT, Lowe TC. Paradox of strength and ductility in metals processed by severe plastic deformation. Journal of Materials Research. 2002;**17**:5-8

[13] Valiev RZ, Sergueeva AV, Mukherjee AK. The effect of annealing on tensile deformation behavior of nanostructured SPD titanium. Scripta Materialia. 2003;**49**:669-674

[14] Horita Z, Ohashi K, Fujita T, Kaneko K, Langdon TG. Achieving high strength and high ductility in precipitation-hardened alloys. Advanced Materials 2005;**17**:1599-1602

[15] Sabirov I, Murashkin MYu, Valiev RZ. Nanostructured aluminium alloys produced by severe plastic deformation: new horizons in development. Materials Science and Engineering: A. 2013;**560**:1-24

[16] Zhao Y, Zhu YT, Lavernia EJ. Strategies for improving tensile ductility of bulk nanostructured materials. Advanced Engineering Materials. 2010;**12**:769-778

[17] Ma E. Eight routes to improve the tensile ductility of bulk nanostructured metals and alloys. JOM. 2006;**58**(4):49-53

[18] Parker ER. Materials Data Book for Engineers and Scientists. New York: McGraw-Hill; 1967

[19] Brandes EA, Brook GB. In: Smithells Metals Reference Book, 7th ed. Oxford: Butterworth–Heinemann; 1992 (Chap. 22.)

[20] Valiev RZ. Nanostructuring of metals by severe plastic deformation for advanced properties. Nature Materials. 2004;**3**:511-516

[21] Langdon TG. An evaluation of the strain contributed by grain boundary sliding in superplasticity. Materials Science and Engineering: A. 1994;**174**:225-230

[22] Lee S, Utsunomiya A, Akamatsu H, Neishi K, Furukawa M, Horita Z, Langdon TG. Influence of scandium and zirconium on grain stability and superplastic ductilities in ultrafine-grained Al–Mg alloys. Acta Materialia. 2005;**50**:553-564

[23] Nikulin I, Kaibyshev R, Sakai T. Superplasticity in a 7055 aluminum alloy processed by ECAE and subsequent isothermal rolling. Materials Science and Engineering: A. 2005;**407**:62-70

[24] Kaibyshev R, Shipilova K, Musin F, Motohashi Y. Achieving high strain rate superplasticity in an Al–Li–Mg alloy through equal channel angular extrusion. Materials Science and Technology. 2005;**21**:408-418

[25] Turba K, Ma´lek P, Cieslar M. Superplasticity in an Al–Mg–Zr–Sc alloy produced by equal-channel angular pressing. Materials Science and Engineering: A. 2007;**462**:91-94

[26] Mishra RS, Valiev RZ, McFadden SX, Islamgaliev RK, Mukherjee AK. High-strain-rate superplasticity from nanocrystalline Al alloy 1420 at low temperatures. Philosophical Magazine A. 2001;**81**:37-48

[27] Sakai G, Horita Z, Langdon TG. Grain refinement and superplasticity in an aluminum alloy processed by high-pressure torsion. Materials Science and Engineering: A. 2005;**393**:344-351

[28] Dobatkin SV, Bastarache EN, Sakai G, Fujita T, Horita Z, Langdon TG. Grain refinement and superplastic flow in an aluminum alloy processed by high-pressure torsion. Materials Science and Engineering: A. 2005;**408**:141-146

[29] Xu C, Dobatkin SV, Horita Z, Langdon TG. Superplastic flow in a nanostructured aluminum alloy produced using high pressure torsion. Materials Science and Engineering: A. 2009;**500**:170-175

[30] Sabbaghianrad S, Kawasaki M, Langdon TG. Microstructural evolution and the mechanical properties of an aluminum alloy processed by high-pressure torsion. Journal of Materials Science. 2012;**47**:7789-7795

[31] Kawasaki M, Foissey J, Langdon TG. Development of hardness homogeneity and superplastic behavior in an aluminum-copper eutectic alloy processed by high-pressure torsion. Materials Science and Engineering: A. 2013;**561**:118-125

[32] Alhamidi A, Horita Z. Grain refinement and high strain rate superplasticity in aluminium 2024 alloy processed by high pressure torsion. Materials Science and Engineering: A. 2015;**622**:139-145

[33] Komura S, Horita Z, Furukawa M, Nemoto M, Langdon TG. An evaluation of the flow behavior during high strain rate superplasticity in an Al-Mg-Sc alloy. Metallurgical and Materials Transactions A. 2001;**32**:707-716

[34] Figueiredo RB, Langdon TG. Record superplastic ductility in a magnesium alloy processed by equal-channel angular pressing. Advanced Engineering Materials. 2008;10:37-40

[35] Figueiredo RB, Langdon TG. Fabricating ultrafine-grained materials through the application of severe plastic deformation: a review of developments in Brazil. Journal of Materials Research and Technology. 2012;**1**:55-62

[36] Langdon TG. Fracture processes in superplastic flow. Metal Science. 1982;**16**:175-183

[37] Kawasaki M, Langdon TG. Developing superplasticity and a deformation mechanism map for the Zn-Al eutectoid alloy processed by high-pressure torsion. Materials Science and Engineering: A. 2011;**528**:6140-6145

[38] Kawasaki M, Langdon TG. Grain boundary sliding in a superplastic zinc-aluminum alloy processed using severe plastic deformation. Materials Transactions. 2008;**49**:84-89

[39] Kawasaki M, Langdon TG. Review: Achieving superplastic properties in ultrafine-grained materials at high temperatures. Journal of Materials Science. 2016;**51**:19-32

[40] Kawasaki M, Langdon TG. Principles of superplasticity in ultrafine-grained materials. Journal of Materials Science. 2007;**42**:1782-1796

[41] Gao N, Wang CT, Wood RJK, Langdon TG. Tribological properties of ultrafine-grained materials processed by severe plastic deformation. Journal of Materials Science. 2012;**47**:4779-4797

[42] Archard JF. Contact and rubbing of flat surfaces, Journal of Applied Physics. 1953;**24**: 981-988

[43] Li J, Wongsa-Ngam J, Xu J, Shan D, Guo B, Langdon TG. Wear resistance of an ultrafine-grained Cu-Zr alloy processed by equal-channel angular pressing. Wear. 2015;**326-327**:10-19

[44] Xu J, Wang X, Zhu X, Shirooyeh M, Wongsa-Ngam J, Shan DB, Guo B, Langdon TG. Dry sliding wear of an AZ31 magnesium alloy processed by equal-channel angular pressing, Journal of Materials Science. 2013;**48**:4117-4127

[45] Abd El Aal MI, EI Mahallaw N, Shehata FA, Abd EI Hameed M, Yoon EY, Kim HS. Wear properties of ECAP-processed ultrafine grained Al-Cu alloys. Materials Science and Engineering: A. 2010;**527**:3726-3732

[46] Ortiz-Cuellar E, Hernandez-Rodriguez MAL, García-Sanchez E. Evaluation of the tribological properties of an Al-Mg-Si alloy processed by severe plastic deformation. Wear. 2011;**271**:1828-1832

[47] Moshkovich A, Perfilyev V, Lapsker I, Gorni D, Rapoport L. The effect of grain size on stribeck curve and microstructure of copper under friction in the steady friction state. Tribology Letters. 2011;**42**:89-98

[48] Moshkovich A, Perfilyev V, Gorni D, Lapsker I, Rapoport L. The effect of Cu grain size on transition from EHL to BL regime (Stribeck curve). Wear. 2011;**271**:1726-1732

[49] Gao LL, Cheng XH. Microstructure and dry sliding wear behavior of Cu-10%Al-4%Fe alloy produced by equal channel angular extrusion. Wear. 2008;**265**:986-991

[50] Gao LL, Cheng XH. Effect of ECAE on microstructure and tribological properties of Cu-10%Al-4%Fe alloy. Tribology Letters. 2007;**27**:221-225

[51] Faghihi S, Li D, Szpunar JA. Tribocorrosion behaviour of nanostructured titanium substrates processed by high-pressure torsion. Nanotechnology. 2010;**21**:485703

[52] Wang CT, Gao N, Gee MG, Wood RJK, Langdon TG. Effect of grain size on the microtribological behavior of pure titanium processed by high-pressure torsion. Wear. 2012;**280-281**:28-35

[53] Kim YS, Lee T, Park KT, Kim WJ, Shin DH. Dry sliding wear behavior of commercial purity aluminum and low carbon steel by severe plastic deformation techniques. in: Zhu YT, Langdon TG, Mishra RS, Semiatin SL, Saran MJ, Lowe TC, editors. Ultrafine Grained Materials II. USA: John Wiley & Sons, Inc.; 2013. pp. 409-418

[54] Wang CT, Gao N, Wood RJK, Langdon TG. Wear behavior of an aluminum alloy processed by equal-channel angular pressing. Journal of Materials Science. 2011;**46**:123-130

[55] Padap AK, Chaudhari GP, Nath SK. Mechanical and dry sliding wear behavior of ultrafine-grained AISI 1024 steel processed using multiaxial forging. Journal of Materials Science. 2010;**45**:4837-4845

[56] Purcek G, Saray O, Kul O, Karaman I, Yapici GG, Haouaoui M, Maier HJ. Mechanical and wear properties of ultrafine-grained pure Ti produced by multi-pass equal-channel angular extrusion. Materials Science and Engineering: A. 2009;**517**:97-104

[57] Valiev RZ, Islamgaliev RK, Alexandrov IV. Bulk nanostructured materials from severe plastic deformation. Progress in Materials Science. 2000;**45**:103-189

[58] Valiev RZ, Estrin Y, Horita Z, Langdon TG, Zehetbauer MJ, Zhu YT. Producing bulk ultrafine-grained materials by severe plastic deformation. JOM. 2006;**58**(4):33-39

[59] Geiger M, Kleiner M, Eckstein R, Tiesler N, Engel U. Microforming. CIRP Annals—Manufacturing Technology. 2001;**50**:445-462

[60] Engel U, Eckstein R. Microforming—From basic research to its realization. Journal of Materials Processing Technology. 2002;**35**:125-126

[61] Vollertsen F, Niehoff HS, Hu Z. State of the art in micro forming. International Journal of Machine Tools and Manufacture. 2006;**46**:1172-1179

[62] Vollertsen F, Biermann D, Hansen HN, Jawahir IS, Kuzman K. Size effects in manufacturing of metallic components. CIRP Annals—Manufacturing Technology. 2009;**58**:566-587

[63] Fu MW, Chan WL. A review on the state-of-the-art microforming technologies. International Journal of Advanced Manufacturing Technology. 2013;**67**:2411-2437

[64] Janssen PJM, De Keijser TH, Geers MGD. An experimental assessment of grain size effects in the uniaxial straining of thin Al sheet with a few grains across the thickness. Materials Science and Engineering: A. 2006;**419**:238-248

[65] Estrin Y, Janecek M, Raab GI, Valiev RZ, Zi A. Severe plastic Deformation as a means of producing ultra-fine-grained net-shaped micro electro-mechanical systems parts. Metallurgical and Materials Transactions A. 2007;**38**:1906-1909

[66] Zhilyaev AP, Langdon TG. Using high-pressure torsion for metal processing: Fundamentals and applications. Progress in Materials Science. 2008;**53**:893-979

[67] Kwan CCF, Wang Z. Cyclic deformation of ultra-fine grained commercial purity aluminum processed by accumulative roll-bonding. Materials. 2013;**6**:3469-3481

[68] Kim WJ, Sa YK. Micro-extrusion of ECAP processed magnesium alloy for production of high strength magnesium micro-gears. Scripta Materialia. 2006;**54**:1391-1395

[69] Ma X, Lapovok R, Gu C, Molotnikov A, Estrin Y, Pereloma EV, Davies CHJ, Hodgson PD. Deep drawing behaviour of ultrafine grained copper: modelling and experiment. Journal of Materials Science. 2009;**44**:3807-3812

[70] Xu J, Zhu X, Shi L, Shan D, Guo B, Langdon TG. Micro-forming using ultrafine-grained aluminum processed by equal-channel angular pressing. Advanced Engineering Materials. 2015;**636**:3527-360

[71] Xu J, Shi L, Wang C, Shan D, Guo B. Micro hot embossing of micro-array channels in ultrafine-grained pure aluminum using a silicon die. Journal of Materials Processing Technology. 2015;**225**:375-384

[72] Yu CY, Sun PL, Kao PW, Chang CP. Mechanical properties of submicron-grained aluminum. Scripta Materialia. 2005;**52**:359-363

[73] Sabirov I, Barnett MR, Estrin Y, Hodgson PD. The effect of strain rate on the deformation mechanisms and the strain rate sensitivity of an ultra-fine-grained Al alloy. Scripta Materialia. 2009;**61**:181-184

[74] Wang M, Shan A. Effect of strain rate on the tensile behavior of ultra-fine grained pure aluminum. Journal of Alloys and Compounds. 2008;**455**:L10-L14

[75] Le GM, Godfrey A, Hansen N, Liu W, Winther G, Huang X. Influence of grain size in the near-micrometre regime on the deformation microstructure in aluminium. Acta Materialia. 2013;**61**:7072-7086

[76] Okamoto NL, Kashioka D, Hirato T, Inui H. Specimen- and grain-size dependence of compression deformation behavior in nanocrystalline copper. International Journal of Plasticity. 2014;**56**:173-183

[77] Xu J, Zhu X, Shan D, Guo B, Langdon TG. Effect of grain size and specimen dimensions on micro-forming of high purity aluminum. Materials Science and Engineering: A. 2015;**646**:207-217

[78] Xu J, Li J, Zhu X, Fan G, Shan D, Guo B. Microstructural evolution at micro/meso-scale in an ultrafine-grained pure aluminum processed by equal-channel angular pressing with subsequent annealing treatment. Materials. 2015;**8**:7447-7460

[79] Rosochowski A, Presz W, Olejnik L, Richert M. Micro-extrusion of ultra-fine grained aluminium. International Journal of Advanced Manufacturing Technology. 2007;**33**:137-146

[80] Zhao YH, Guo YZ, Wei Q, Dangelewicz AM, Xu C, Zhu YT, Langdon TG, Zhou YZ, Lavernia EJ. Influence of specimen dimensions on the tensile behavior of ultrafine-grained Cu. Scripta Materialia. 2008;**59**:627-630

[81] Zhao YH, Guo YZ, Wei Q, Topping TD, Dangelewicz AM, Zhu YT, Langdon TG, Lavernia EJ. Influence of specimen dimensions and strain measurement methods on tensile stress-strain curves. Materials Science and Engineering: A. 2009;**525**:68-77

[82] Kim WJ, Yoo SJ, Kim HK. Superplastic microforming of Mg-9Al-1Zn alloy with ultrafine-grained microstructure. Scripta Materialia. 2008;**59**:599-602

[83] Xu J, Xing X, Shan D, Guo B, Langdon TG. An evaluation of formability using micro-embossing on an ultrafine-grained magnesium AZ31 alloy processed by high-pressure torsion. MATEC Web of Conference. 2015;**21**:09005

[84] Xu J, Shi L, Wang C, Shan D, Guo B. Micro hot embossing of micro-array channels in ultrafine-grained pure aluminum using a silicon die. Journal of Materials Processing Technology. 2015;**225**:375-384

[85] Xu J, Zhu X, Shi L, Shan D, Guo B, Langdon TG. Advanced Engineering Materials. 2015;**17**:1022-1033

[86] I. Sabirow, N.A. Enikeev, M. Yu. Murashkin, R.Z. Valiev. Bulk Nanostructured Materials with Multifunctional Properties. Springer; 2015. Switzerland, 125 p

[87] www.timplant.cz

[88] Valiev RZ, Semenova IP, Latysh VL, Rack H, Lowe TC, Petruzelka J, Dluhos L, Hrusak D, Sochova J. Nanostructured titanium for biomedical applications. Advanced Engineering Materials. 2008;**10**:B15-B17

[89] Mishnaevsky Jr L, Levashov E, Valiev RZ, Segurado J, Sabirov I, Enikeev N, Prokoshkin S, Solov'yov AV, Korotitsky A, Gutmanas E, Gotman I, Rabkin E, Psakh'e S, Dluhos L, Seefeldt M, Smolin A. Nanostructured titanium-based materials for medical implants: modeling and development. Materials Science and Engineering: R. 2014;**81**:1-19

[90] Cubero-Sesin JM, In H, Arita M, Iwaoka H, Horita Z. High-pressure torsion for fabrication of high-strength and high-electrical conductivity Al micro-wires. Journal of Materials Science. 2014;**49**:6550-6556

[91] Champion Y, Brechet Y. Effect of grain size reduction and geometrical confinement in fine grained copper: Potential applications as a material for reversible electrical contacts. Advanced Engineering Materials. 2010;**12**:798-802

[92] Azushima A, Kopp R, Korhonen A, Yang DY, Micari F, Lahoti GD, Groche P, Yanagimoto J, Tsuji N, Rosochowski A, Yanagida A. Severe plastic deformation (SPD) processes for metals. CIRP Annals—Manufacturing Technology. 2008;**57**:716-735

[93] Safiullin AR, Safiullin RV, Kruglov AA. Application of nanostructured Ti alloys for producing a face for a gold club. Reviews on Advanced Materials Science. 2010;**25**:281-285